

Selected Paper

Luminescence of Sn²⁺ Center in ZnO–B₂O₃ Glasses Melted in Air and Ar ConditionsHirokazu Masai,^{*1} Yuto Suzuki,¹ Takayuki Yanagida,² and Ko Mibu³¹Institute for Chemical Research, Kyoto University, Gokasho, Uji, Kyoto 611-0011²Nara Institute of Science and Technology, 8916-5 Takayama, Ikoma, Nara 630-0101³Department of Engineering Physics, Electronics, and Mechanics, Graduate School of Engineering, Nagoya Institute of Technology, Gokiso-cho, Showa-ku, Nagoya, Aichi 466-8555

E-mail: masai.h@scl.kyoto-u.ac.jp

Received: April 22, 2015; Accepted: May 12, 2015; Web Released: May 18, 2015

The authors report on luminescence of SnO-doped 60ZnO–40B₂O₃ (SZB) glasses melted in air and Ar atmosphere. In photoluminescence (PL), excitation spectra consist of two excitation bands, and the lower excitation band, emerging at lower energy with increasing amount of SnO, affects the optical absorption edge. The present SZB glasses can exhibit light emission by irradiation of near UV light, which is different from the zinc phosphate glass system. X-ray induced scintillation spectra indicate that concentration of Sn²⁺ mainly affects the intensity. ¹¹⁹Sn Mössbauer spectra show that a certain amount of Sn²⁺ centers in the SZB glass was oxidized to Sn⁴⁺ even when melted under the inert atmosphere, which is one of the reasons for the low PL quantum efficiencies, approximately 60%. The ¹¹⁹Sn Mössbauer spectra also suggest site dispersion of Sn²⁺ centers, whose local coordination states affect the optical absorption and luminescent properties.

Oxide glasses possessing transparency, chemical durability, and wide chemical composition range are one of the fundamental materials in our daily lives. Because glasses have no structural ordering in the long range, the good formability is also an advantage for practical applications. Although such oxide glasses generally exhibit little light emission without a strong laser light source, fiber-type lasers using glass-based devices have been used by doping with rare earth (RE) cations possessing a sharp emission band. On the contrary, non-rare earth cations exhibiting light emission have attracted attention not only from ubiquitous presence but also from unique emission properties. The *ns*²-type cation (*n* ≥ 4) is an emission center that gives strong photoluminescence (PL) because of the parity allowed transition.^{1,2} The emission centers, such as Sn²⁺, Sb³⁺, Tl⁺, and Pb²⁺, which possess electrons in the outermost shell in both the ground state (*ns*²) and the excited state (*ns*¹*np*¹), exhibit a broad emission with a lifetime of the microsecond order,¹ and the PL intensity of the emission center is generally stronger than that of transition metal emission centers whose emission is inherently forbidden. For example, Sb³⁺, Mn²⁺-codoped halo-calcium phosphate crystal has been used for practical white fluorescent lamps,^{1,3} and several authors have been focused on the *ns*²-type centers in glass.^{4–13}

Recently, the authors reported PL of Sn²⁺-doped ZnO–P₂O₅ low-melting glasses.^{9–12} The glasses showed blue light emission with high quantum efficiency (QE) by deep UV irradiation. It is notable that the transparent Sn²⁺-containing glasses show intense UV-excited emission comparable to crystal

phosphor. In addition, we have also demonstrated white light emission from MnO-codoped SnO–ZnO–P₂O₅ glasses using energy transfer from Sn²⁺ to Mn²⁺ centers.¹⁰ Thus, the emission consisting of broad bands can be tailored by addition of another emission center, or by changing the local coordination field of the Sn²⁺ center (i.e. by changing chemical composition of the mother glasses). On the other hand, radioluminescence (RL) properties of the same glass system have been reported.^{13,14} More recently, we have demonstrated UV-excited light emission of Sn²⁺-doped strontium borate glasses, and discussed the energy diagram by comparison with oxide crystal possessing stoichiometric chemical composition.¹⁵ In a previous report,¹⁵ it was found that borate systems can also exhibit high QE values around 80%. From these reports, we have emphasized that the Sn²⁺ center is a fascinating non-RE center in glasses.

In the present study, we examined luminescence of Sn-doped zinc borate glasses by UV and X-ray irradiation. Various kinds of ZnO–B₂O₃ glasses have been examined as a host material for luminescent applications.^{16–21} Although it is easily expected that zinc borate glasses can be a good host of the Sn²⁺ center for PL and RL applications, the number of previous reports on Sn²⁺ in zinc borate glasses is limited. It therefore follows that examination of the luminescence is worthwhile. Here, the chemical composition of the mother glass was selected as 60ZnO–40B₂O₃ for comparison with the previous phosphate 60ZnO–40P₂O₅ system.^{9,22} To examine the effect of basicity of oxide matrix on the emission properties of the Sn²⁺ emission

center is also meaningful from the viewpoint of the local structure in the glass matrix. In order to clarify the oxidation reaction during the melting in air, we have prepared zinc borate glasses melted in air and Ar. By studying the luminescence properties of the glasses, this report provides a valuable guideline for preparation of activator-doped inorganic borate glasses by melt quenching.

Experimental

The $x\text{SnO}-(60-x)\text{ZnO}-40\text{B}_2\text{O}_3$ ($x\text{SZB}$) glasses were prepared according to a conventional melt quenching method using a platinum crucible.²² Batches consisting of SnO (99.5%), ZnO (99.9%), and B_2O_3 (99.9%), which were purchased from Kojundo Chemical Laboratory Co., Ltd. and stored in a desiccator, were mixed and melted at 1100 °C for 30 min in air and Ar (99.999%) atmosphere. The glass melt was quenched on a stainless plate maintained at 200 °C and then annealed at the glass-transition temperature, T_g , as measured by differential thermal analysis (DTA), for 1 h. After cutting (10 mm × 10 mm × 1 mm), the glass samples were polished with aqueous diamond slurries. Because the sample size for measurement was fixed, we can quantitatively compare the luminescence intensity among these samples.

The absorption spectra were measured using an U3500 UV-vis-NIR spectrophotometer (Hitachi, Japan). The PL and PL excitation (PLE) spectra were measured at room temperature using an F7000 fluorescence spectrophotometer (Hitachi, Japan). On PL measurements, band pass filters were used for the excitation (2.5 nm) and the emission (2.5 nm). The emission decay at room temperature was measured using a Quantaurs-Tau (Hamamatsu Photonics, Japan). The excitation light source for emission decay measurement was an LED operated at a photon energy of 4.43 eV and a frequency of 10 kHz. The internal quantum efficiency (QY) was evaluated using a Quantaurs-QY (Hamamatsu Photonics, Japan). RL spectra by X-ray radiation at room temperature were measured using the monochromator equipped charge coupled device (CCD, Andor DU-420-BU2).²³ The supplied bias voltage and tube current were 40 kV and 0.052–5.2 mA, respectively. The irradiated dose was calibrated by using an ionization chamber. ¹¹⁹Sn Mössbauer spectra, i.e., absorption spectra of γ -rays by the ¹¹⁹Sn nuclei in the samples, were measured in conventional transmission geometry using a $\text{Ca}^{119\text{m}}\text{SnO}_3$ source at room temperature. The energy of the γ -rays from the source was modulated by the Doppler effect using a velocity transducer with a constant acceleration mode, and the abscissa of the spectra was expressed with the unit of the Doppler velocity as in the literature. The valence states of the Sn atoms, which are sensitively reflected as the peak positions in ¹¹⁹Sn Mössbauer spectra,²⁴ were deduced by fitting the measured spectra using standard software Normos (made by R. A. Brand, commercially available from WissEl GmbH).

Results and Discussion

PL Properties of $x\text{SZB}$ Glasses Melted in Air and in Ar.

In the composition range of $x = 0$ –2.0, the obtained $x\text{SZB}$ glasses were colorless and transparent independently of the preparing atmosphere. Figure 1 shows the DTA curves of the $x\text{SZB}$ glasses with varying Sn contents. The values of T_g for

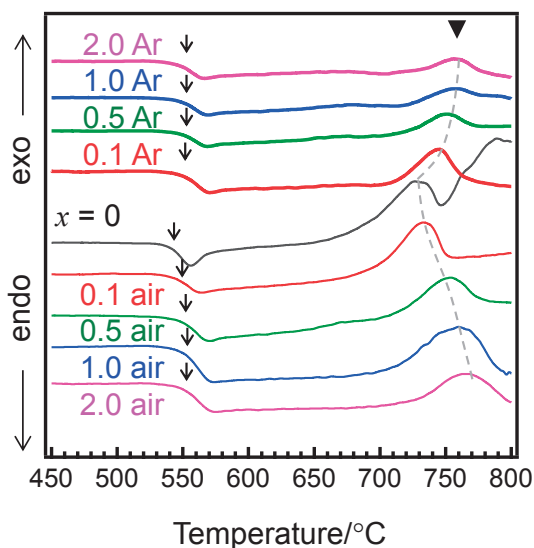


Figure 1. Powder DTA patterns of the $x\text{SZB}$ glasses with varying Sn contents. T_g of each sample is shown using arrows. Triangle and dashed line indicate the first crystallization peak of each glass.

these glasses were in the range of 545 ± 3 °C, and no significant difference was observed in T_g based on the chemical compositions. We can find that temperature of the first crystallization peak T_p increases with increasing amount of Sn as shown in Figure 1. The quantity ΔT , $T_p - T_g$, is defined as the thermal stability parameter for crystallization of the glass. The change of ΔT indicates that the glass network is stabilized by addition of SnO. Figure 2a shows the optical absorption spectra of $x\text{SZB}$ glasses ($x = 0, 0.1, 0.5, 1.0, \text{ and } 2.0$) melted in air. Since the origin of the absorption edge is Sn^{2+} cation (intra-atomic $5s^2-5s^15p^1$ transition), we hereby treat as a direct transition.²⁵ The absorption edge is red-shifted with increasing the amount of SnO. It was found that the absorption edge of the SnO-doped oxide glasses correlated with the local coordination state of the Sn^{2+} emission center.^{11,12} Based on the previous reports,^{11,24} we introduce the optical band edge $E_{g, \text{opt}}$ which is evaluated by the extrapolation of the linear portion of the absorption spectra as shown in Figure 2a. Figure 2b shows the differential $E_{g, \text{opt}}$ ($\Delta E_{g, \text{opt}}$) values from the nondoped glass as a function of Sn amount. By fitting an exponential function, it is found that the slope of $\Delta E_{g, \text{opt}}$ of the $x\text{SZB}$ glasses melted in Ar is 1.3 times steeper than that of the glasses melted in air. In our previous reports,¹² we have found that the shift of optical absorption also correlates with the actual concentration of the Sn^{2+} center, and that almost 100% of tin species can exist as Sn^{2+} valence states in $\text{ZnO}-\text{P}_2\text{O}_5$ glasses melted under Ar. Therefore, it suggests that the observed difference between the glass melted in Ar and one melted in air is due to the real amount of Sn^{2+} center in each glass, and it also indicates an oxidation reaction of Sn^{2+} into Sn^{4+} during the melting in air.

Figure 3 shows the PL-PLE contour plots of the $x\text{SZB}$ glasses: $x = 0.1$ and 1.0 using an intensity axis on a linear scale. These intensities are normalized using the peak in order to compare these spectrum shapes. The PL peak intensities of the $x\text{SZB}$ glasses melted in Ar are approximately 1.2 times as

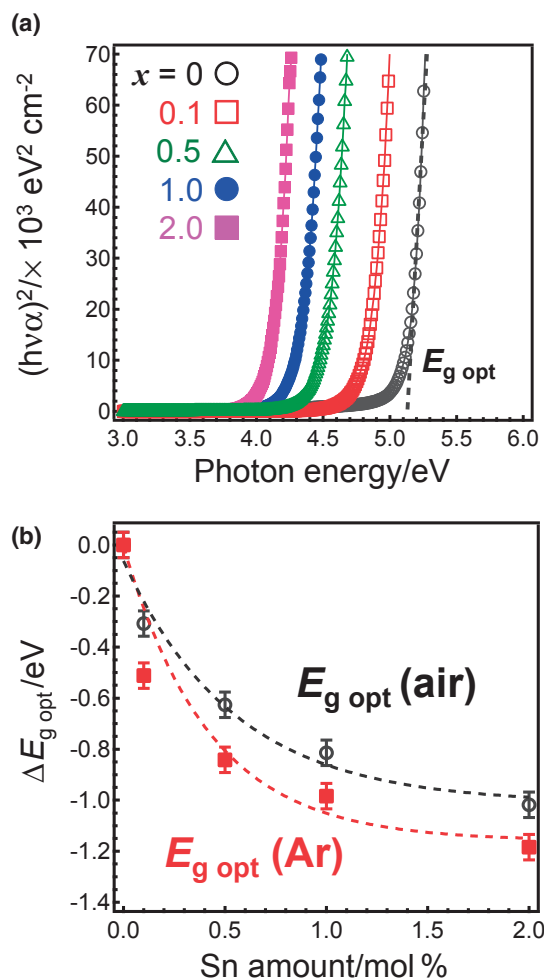


Figure 2. (a) Optical absorption spectra of x SZB glasses ($x = 0, 0.1, 0.5, 1.0,$ and 2.0) melted in air. (b) Differential $E_{g \text{ opt}}$ ($\Delta E_{g \text{ opt}}$) values from the nondoped ZB glass as a function of Sn amount.

large as those of the glasses melted in air. As shown in Figure 3, an additional PLE band appears in the excitation in the lower energy region in the x SZB glasses melted in Ar, and the intensity is enhanced by the inert preparation. These figures indicate that the higher the excitation energy becomes, the higher the emission peak energy becomes. The intensity of the emission takes the maximum at a composition of $x = 1.0$, which is much larger in comparison with SnO-doped strontium borate glass system containing 75 mol % of B_2O_3 .¹⁵ Although the present divalent cation, Zn^{2+} , is different from that in the previous report (Sr^{2+}), we can speculate that the network forming B_2O_3 concentration affects the dispersion of dopant cation. Future study is needed to examine the correlation between chemical composition and dispersion of doped emission centers.

In all chemical compositions, emission intensity of PL-PLE spectra of the SZB glass melted in Ar was higher than that of the glass melted in air. Normalized PL-PLE spectra of the 0.1SZB glasses prepared in different atmospheres are shown in Figure 4a. The PL spectra were obtained by excitation of the peak energy of PLE spectra whereas the PLE spectra were

obtained by scanning of the peak energy of PL spectra. Although band overlap of PL and PLE is observed around 3.5 eV, we confirm that the SZB glass shows light emission by near-UV light (365 nm) shown in Figure 4b. Because no emission was observed in the zinc phosphate system in the same irradiation condition, it is an advantage of the borate glasses in comparison with phosphate glasses. Figure 4c shows the concentration dependence of peak energies of PL and PLE bands of the SZB glasses. With increasing Sn amount, both the excitation peaks and the emission peaks red-shift. Comparing Figure 4c with optical absorption edge shown in Figure 2b, we have found that the change of PLE peak does not correspond to the change of the optical absorption edge. Such correlation between the optical absorption edge and the PLE peak was observed in the $SrO-B_2O_3$ glass system,¹⁵ but not observed in the $ZnO-P_2O_5$ glass system.^{9,11,12} Thus, we think that the emergence of excitation band at lower photon energy by addition of SnO, whose intensity is lower than that of the excitation peak band, is characteristic of the borate glass system. Based on the obtained results as shown above, the emerging band affects the optical absorption edge and the light conversion of near-UV light, which is different from the phosphate glass system.

The emission decay curves monitored at 2.95 eV for the x SZB glasses melted in air are shown in Figure 5, where the samples were irradiated using UV light of 4.43 eV. It was reported that the Sn^{2+} center possessing C_{2v} symmetry in SiO_2 glass exhibits the S_1 excitation band at 4.9 eV.⁶ On the other hand, we recently reported that the higher-energy band is due to 2-coordinated Sn^{2+} whereas the lower band is due to Sn^{2+} center possessing high coordination number in phosphate glass.¹² The decay curves consist of two components: one is faster (lifetime, $\tau'_{1/e}$, of nanoseconds), and the other is slower ($\tau''_{1/e}$ of microseconds). Considering previous decay constants of the Sn^{2+} center in oxide crystals or oxide glasses, the shown decay with the order of lifetimes of microseconds is due to the $T_1 \rightarrow S_0$ radiative transition, and the $\tau_{1/e}$ lifetime is calculated as ca. $5.8 \pm 0.2 \mu s$, which is almost independent of the SnO amount. The decay constant is comparable to that in other borate glass system.¹⁵ On the other hand, the origin of faster decay is not clarified. Because a lifetime of the F^+ or F center in oxide glasses is reported to be ca. 10^{-2} – 10 s,^{26,27} the possibility is negligible. Although the details have not been clarified yet, plausible origins are (1) the defect center in the host zinc borate glass,²¹ or (2) S_1 - S_0 relaxation of the Sn^{2+} center.^{1,15}

Figure 6 shows the relationship between the SnO concentration and internal quantum efficiency (QE) of the x SZB glasses melted in air and in Ar. The magnitudes of the glasses melted in Ar are higher than that melted in air, and the QE values of the glass melted in Ar atmosphere are around 60%, and slightly decrease in the case of 2.0 mol % addition. It is notable that the maximum QE values of the $ZnO-B_2O_3$ glasses are at least 20% lower than those of $ZnO-P_2O_5$ glasses.¹¹ On the other hand, the zinc borate system can possess light emission by excitation of near-UV light (365 nm), although the efficiency is not so large. Although the mechanism has not been clarified yet, one of the plausible reasons is the basicity of the host matrix which affects the radiative/nonradiative relaxation rates.

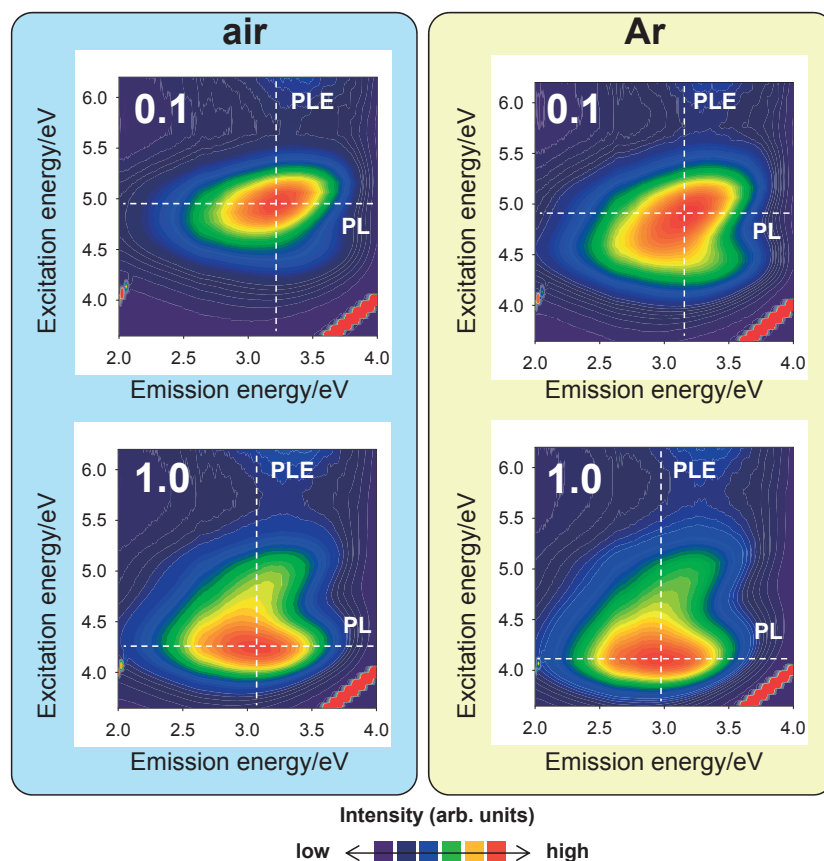


Figure 3. PL-PLE 3D contour plots of the *x*SZB glasses prepared in air and Ar. Intensities are normalized using the peak intensity in order to compare these spectra shapes. Dashed lines indicate the peak energies of each excitation and emission energy.

X-ray-Induced Scintillation Properties of *x*SZB Glasses Melted in Air and in Ar. It was reported that Sn²⁺-doped oxide glasses exhibit scintillation by X-ray irradiation.^{13,14} Therefore, it is natural to assume that the present zinc borate glasses also show the emission. Figure 7a shows X-ray-induced scintillation spectra of the *x*SZB glasses (*x* = 0, 0.1, 0.5, 1.0, and 2.0) melted under Ar. In Sn-free glass, broad emission attributable to defects in the glass is observed. On the other hand, the broad emission due to Sn²⁺ centers is observed from Sn²⁺-doped samples. The peak energies of the *x*SZB glasses prepared in both conditions are red-shifted with increasing Sn amount, corresponding to the PL peak shift shown in Figure 4b. Although the peak energies of scintillation are similar to those of PL, which suggests the emission-related energy levels of PL and scintillation are the same, the emission intensity roughly increases with increasing the SnO amount. Thus, in the X-ray-induced scintillation process, in which secondary electrons generated from the host matrix by the exposure activate the Sn²⁺ centers, the highest scintillation intensity was obtained from the *x*SZB glasses containing much higher SnO amount in comparison with that in the PL process even though some concentration quenching may occur. Figure 7b shows the correlation between the irradiated dose and the scintillation intensity of the *x*SZB glasses melted in Ar. In the Sn²⁺ concentration range (0 ≤ *x* ≤ 2), a linear dependence of the absorbed dose is observed, suggesting a considerable defect is not generated in the glass during the X-ray

irradiation. On the other hand, Figure 7c shows the correlation between the scintillation intensity and additive amount of the Sn species in the glasses. There is a deviation from the linear dependence of the emission intensity at higher Sn-added region. The deviation from the linear change suggests the concentration quenching of the Sn²⁺ center. It is found that (1) values of $E_{g\text{ opt}}$ reflect the Sn²⁺ concentration,¹² and (2) scintillation intensity also depends on the concentration of activator,²⁸ whose concentration quenching occurred in higher amount compared with the photoluminescence process. Therefore, we focus on the relationship between $E_{g\text{ opt}}$ and scintillation intensity in order to estimate the amount of Sn²⁺ center in the SZB glass. Figure 7d shows correlation between the scintillation intensity and $E_{g\text{ opt}}$ of the SZB glasses prepared in Ar. It has been previously suggested that the value of $E_{g\text{ opt}}$ can be a standard for evaluation of Sn²⁺ species.¹¹ As shown in Figure 7d, there is a linear relationship between the scintillation intensity and $E_{g\text{ opt}}$. The correlation also suggests that X-ray-induced scintillation intensity of the SZB glasses is mostly governed by the amount of Sn²⁺ emission center.

Relationship between Sn²⁺ Concentration of *x*SZB Glasses and the Luminescence. In order to examine the correlation between the real Sn²⁺ content and optical properties in these glasses, we evaluate the valence state of tin using ¹¹⁹Sn Mössbauer spectroscopy. Figure 8a shows ¹¹⁹Sn Mössbauer spectra of the 1SZB glasses prepared in air and in Ar along with that of the 0.1SZB glass prepared in Ar. The peaks

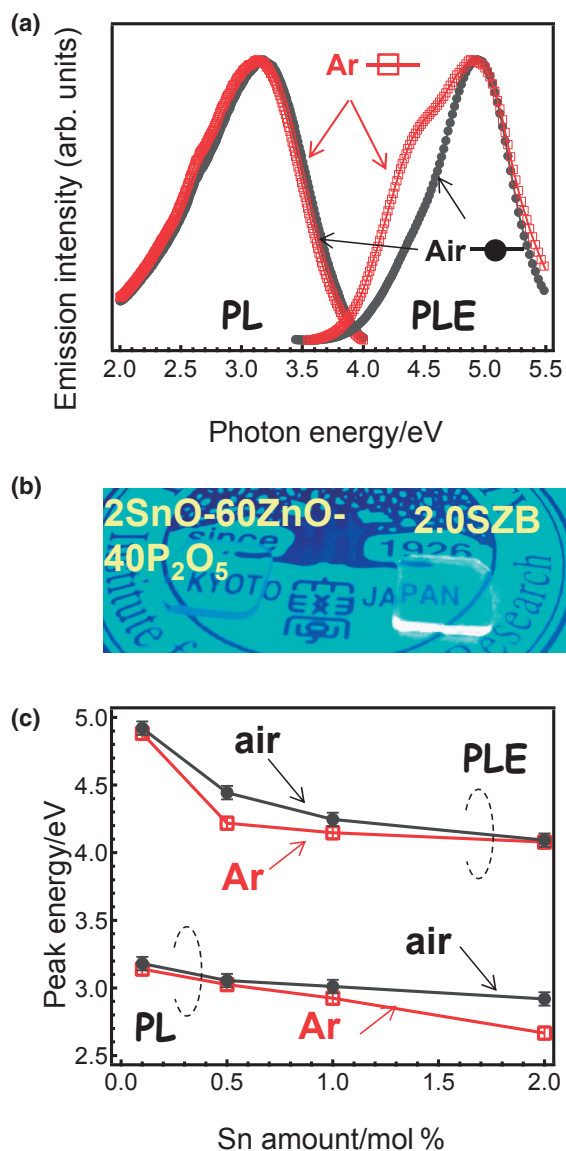


Figure 4. (a) Normalized PL-PLE spectra of 0.1SZB glasses prepared in air and Ar. The PL spectra were obtained by excitation of the peak energy of PLE spectra whereas the PLE spectra were obtained by scanning the peak energy of PL spectra. (b) Photograph of 2.0SZB glass together with 2SnO–60ZnO–40P₂O₅ glass under UV (365 nm) irradiation. (c) Concentration dependence of peak energies of PL and PLE bands of the SZB glasses as a function of Sn amount.

around 0 mm s^{-1} correspond to the Sn⁴⁺ species, whereas those around 2 and 4 mm s^{-1} correspond to the Sn²⁺ species.²⁹ These spectra show that certain amounts of Sn²⁺ in these glasses were oxidized to Sn⁴⁺, even though the glass was melted in an inert atmosphere. After peak deconvolution, the Sn²⁺ ratios of the 1SZB glass melted in air and that melted in Ar are calculated to be 14%, and 45%, respectively. On the other hand, if correction of Debye–Waller factors (Sn²⁺: 0.22, and Sn⁴⁺: 0.49)^{12,30} are applied, the Sn²⁺ ratios of these glasses become 26%, and 65%, respectively. It is notable that approximately a half of Sn²⁺ centers were oxidized during inert melting, even after the

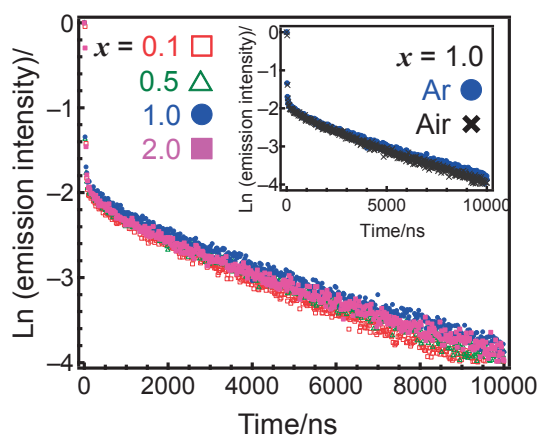


Figure 5. PL decay curves of the *x*SZB glasses melted in Ar. Inset shows PL decay curves of the 0.5SZB glasses prepared in Ar and air.

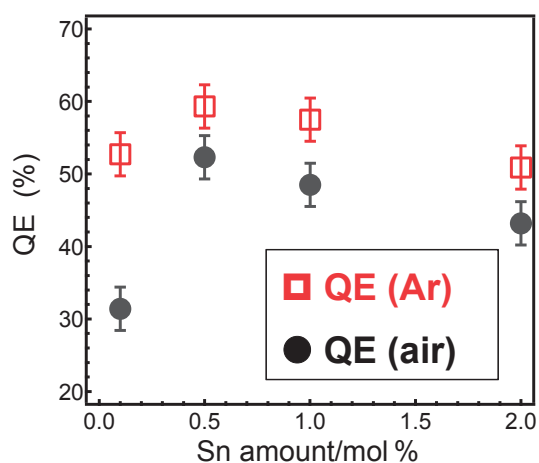


Figure 6. QE values of the *x*SZB glasses prepared in air and Ar as a function of Sn amount.

correction factors. Considering the purity of Ar gas (99.999%), the purged melting condition, and previous studies on zinc phosphate glass system, we speculate about plausible reasons that (1) the basicity of glass affects the Sn²⁺/Sn⁴⁺ ratio and/or (2) the starting materials contain an oxidation component. Since the optical basicity of B₂O₃ and P₂O₅ are 0.42, and 0.33, respectively,³¹ we hereby think that the origin is mainly attributable to basicity of the host glass, and that the low Sn²⁺ concentration is one of the origins of the lower QE values (Figure 6) in comparison with a zinc phosphate system. However, another possibility cannot be denied, because the 0.1SZB glass prepared under Ar contained Sn²⁺ ratio of 23% (40% by using the correction factors). Since the values of basicity of these host glasses take similar values, the Sn²⁺ ratio of these glasses under Ar preparation suggests a hypothesis that some cation-free components were contained in the starting materials to affect the valence state of tin. Although it is not clarified yet, one plausible factor is a hydroxyl group (like as H₃BO₃) or H₂O molecules connected to B₂O₃, because no clear contamination could be observed in the glass system. Since we have used commercially available B₂O₃ powder without any heat

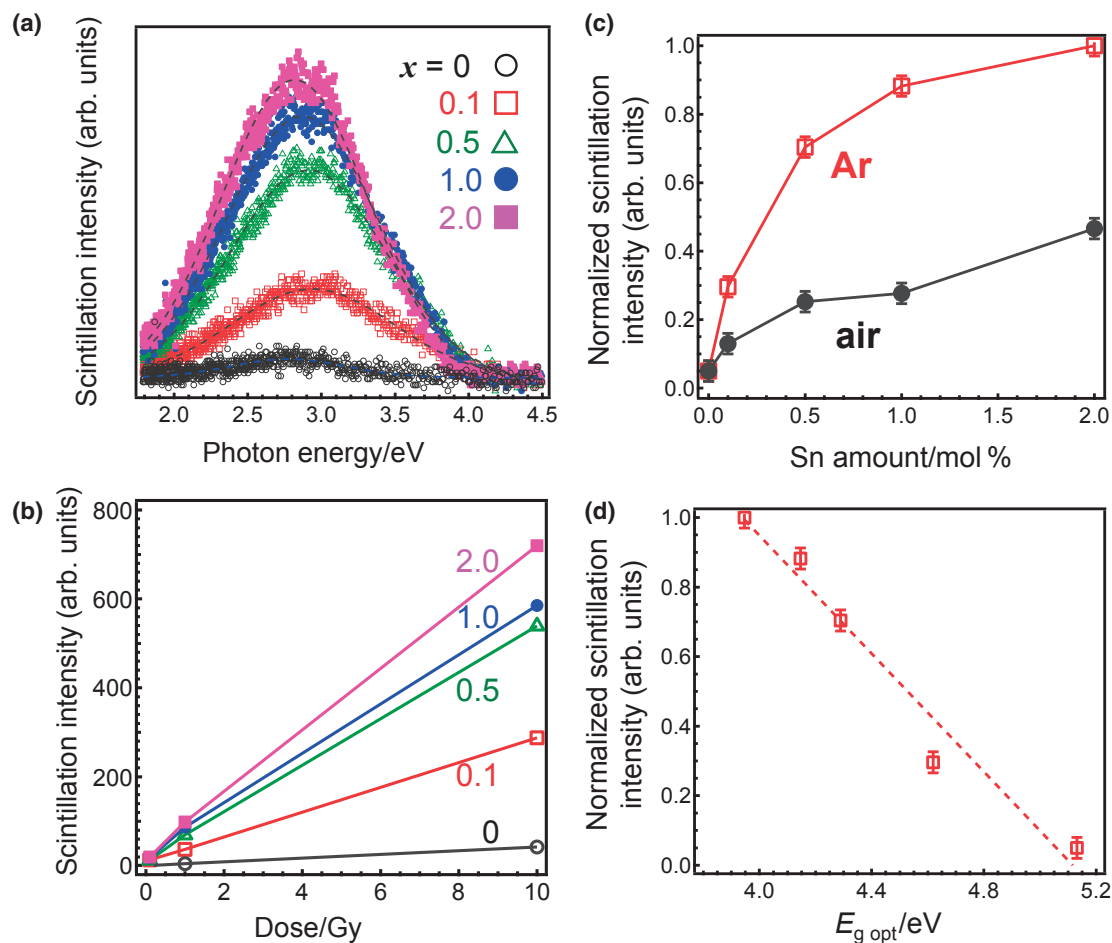


Figure 7. (a) X-ray-induced scintillation spectra of the x SZB glasses prepared under Ar. The dose was 1 Gy. (b) Correlation between the scintillation intensity and the irradiated dose of the x SZB glasses prepared in Ar. (c) Normalized scintillation intensities of the x SZB glasses as a function of Sn amount. The dose of X-ray was 1 Gy. (d) Correlation between the scintillation intensity and $E_{g\text{ opt}}$ of the x SZB glasses prepared in Ar.

treatment, it is expected that OH group or H₂O of starting materials may affect the valence of tin. Here, we have emphasized that the quadrupole doublet of Sn²⁺ in the 1.0SZB glasses is depicted as an asymmetric shape. Since the Sn²⁺ center possess no specific crystallographic orientation in the random glass network, we fitted the spectrum with an assumption that there are two Sn²⁺ sites in the 1.0SZB glasses, whereas only one Sn²⁺ site is observed in the 0.1SZB glass. It is reported that at least two different sites exist in the SnO–ZnO–P₂O₅ glasses.¹² As shown in Figure 4a, an emergence of an excitation band suggests the possibility of additional Sn²⁺ sites. It is, therefore, suggested that the asymmetric peaks attributable to Sn²⁺ species reflect the different local coordination states. Figure 8b shows normalized scintillation intensity and $E_{g\text{ opt}}$ of the SZB glasses melted in Ar shown in Figure 8a as a function of the Sn²⁺ amount, which is obtained by ¹¹⁹Sr Mössbauer analysis without the correction of the Debye–Waller factors. Although the Sn²⁺ amount may be underestimated, the relationship between scintillation intensity and $E_{g\text{ opt}}$ can be discussed. Both scintillation energy and value of $E_{g\text{ opt}}$ are rapidly changed at low concentration, and the degree of increase becomes gradual with increasing the amount of Sn²⁺. Such saturation

curves correspond to an emerging of different coordination states, whose existence is suggested by the results of optical absorption, PL, and Mössbauer spectroscopy.

Conclusion

We have demonstrated the UV-excited photoluminescence and X-ray-induced scintillation of Sn²⁺-doped zinc borate (SZB) glasses. It is found that oxidation of Sn²⁺ to Sn⁴⁺ during glass melting can be detected from the optical absorption edge $E_{g\text{ opt}}$. Although PL characteristic of the Sn²⁺ center in borate glasses was observed, the PL of the zinc borate glasses is different from that of zinc phosphate glasses from the viewpoint of peak energy shift and the potential of luminescence by near UV irradiation. The maximum QE of the present SZB glasses was approximately 60%, which was affected by both Sn²⁺ ratio and basicity of the host glasses. X-ray-induced scintillation intensity of the SZB glasses roughly depends on the real Sn²⁺ amount, which also affects the $E_{g\text{ opt}}$ value. The asymmetric peaks attributable to Sn²⁺ species in ¹¹⁹Sr Mössbauer spectra reflect the different local coordination states of Sn²⁺ species, which is also suggested by other results of the present study.

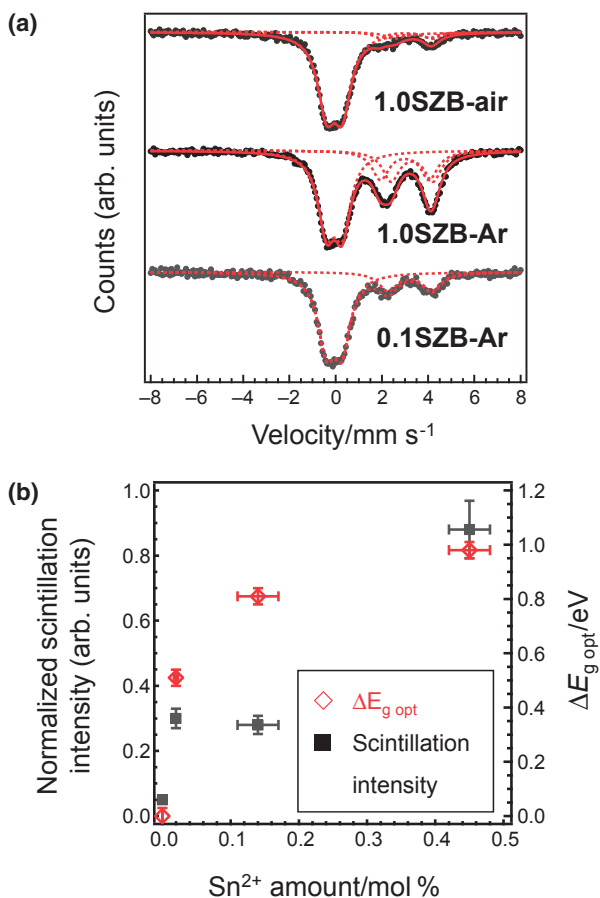


Figure 8. (a) ^{119}Sn Mössbauer spectra of the 1SZB glasses prepared in Ar and air along with that of the 0.1SZB glass prepared in Ar. Dotted lines indicate each Sn component after peak deconvolution. (b) Normalized scintillation intensity and $\Delta E_{\text{g,opt}}$ of the glass melted in Ar as a function of Sn^{2+} amount obtained by Mössbauer spectroscopy.

This work was partially supported by the JSPS KAKENHI Grant-in-Aid for Young Scientists (A) Number 26709048. Collaborative Research Program of I.C.R., Kyoto University (grant #2014-31), and the SPRITS program, Kyoto University. The ^{119}Sn Mössbauer measurement was performed at Nagoya Institute of Technology under the Nanotechnology Platform Program of MEXT, Japan.

References

- 1 S. Tanimizu, in *Phosphor Handbook*, 2nd ed, ed. by W. M. Yen, S. Shionoya, H. Yamamoto, CRC Press, Boca Raton, U.S.A., **2007**, p. 155. doi:10.1201/9781420005233.ch3.
- 2 P. W. M. Jacobs, *J. Phys. Chem. Solids* **1991**, *52*, 35.

- 3 A. Wachtel, *J. Electrochem. Soc.* **1966**, *113*, 128.
- 4 R. Reisfeld, L. Boehm, B. Barnett, *J. Solid State Chem.* **1975**, *15*, 140.
- 5 D. Ehrt, *J. Non-Cryst. Solids* **2004**, *348*, 22.
- 6 L. Skuja, *J. Non-Cryst. Solids* **1992**, *149*, 77.
- 7 T. Hayakawa, T. Enomoto, M. Nogami, *Jpn. J. Appl. Phys.* **2006**, *45*, 5078.
- 8 J. A. Jiménez, *J. Electron. Mater.* **2014**, *43*, 3588.
- 9 H. Masai, Y. Takahashi, T. Fujiwara, S. Matsumoto, T. Yoko, *Appl. Phys. Express* **2010**, *3*, 082102.
- 10 H. Masai, T. Fujiwara, S. Matsumoto, Y. Takahashi, K. Iwasaki, Y. Tokuda, T. Yoko, *Opt. Lett.* **2011**, *36*, 2868.
- 11 H. Masai, T. Tanimoto, T. Fujiwara, S. Matsumoto, Y. Tokuda, T. Yoko, *Opt. Express* **2012**, *20*, 27319.
- 12 T. Masai, T. Tanimoto, S. Okumura, K. Teramura, S. Matsumoto, T. Yanagida, Y. Tokuda, T. Yoko, *J. Mater. Chem. C* **2014**, *2*, 2137.
- 13 H. Masai, T. Yanagida, Y. Fujimoto, M. Koshimizu, T. Yoko, *Appl. Phys. Lett.* **2012**, *101*, 191906.
- 14 H. Masai, Y. Hino, T. Yanagida, Y. Fujimoto, K. Fukuda, T. Yoko, *J. Appl. Phys.* **2013**, *114*, 083502.
- 15 H. Masai, Y. Yamada, Y. Suzuki, K. Teramura, Y. Kanemitsu, T. Yoko, *Sci. Rep.* **2013**, *3*, 3541.
- 16 M. Bettinelli, A. Speghini, M. Ferrari, M. Montagna, *J. Non-Cryst. Solids* **1996**, *201*, 211.
- 17 A. Ivankov, J. Seekamp, W. Bauhofer, *J. Lumin.* **2006**, *121*, 123.
- 18 A. D. Sontakke, A. Tarafder, K. Biswas, K. Annapurna, *Physica B (Amsterdam, Neth.)* **2009**, *404*, 3525.
- 19 G. Pozza, D. Ajó, M. Bettinelli, A. Speghini, M. Casarin, *Solid State Commun.* **1996**, *97*, 521.
- 20 D. Saritha, Y. Markandeya, M. Salagram, M. Vithal, A. K. Singh, G. Bhikshamaiah, *J. Non-Cryst. Solids* **2008**, *354*, 5573.
- 21 H. Masai, Y. Yamada, S. Okumura, Y. Kanemitsu, T. Yoko, *Opt. Lett.* **2013**, *38*, 3780.
- 22 H. Masai, T. Tanimoto, T. Fujiwara, S. Matsumoto, Y. Takahashi, Y. Tokuda, T. Yoko, *J. Non-Cryst. Solids* **2012**, *358*, 265.
- 23 T. Yanagida, K. Kamada, Y. Fujimoto, H. Yagi, T. Yanagitani, *Opt. Mater.* **2013**, *35*, 2480.
- 24 N. N. Greenwood, T. C. Gibb, *Mössbauer Spectroscopy*, Chapman and Hall Ltd., **1971**, Chap. 14. doi:10.1007/978-94-009-5697-1_14.
- 25 J. Tauc, A. Menth, *J. Non-Cryst. Solids* **1972**, *8–10*, 569.
- 26 B. D. Evans, *J. Nucl. Mater.* **1995**, *219*, 202.
- 27 S. Ikeda, T. Uchino, *J. Phys. Chem. C* **2014**, *118*, 4346.
- 28 H. Masai, Y. Hino, T. Yanagida, Y. Fujimoto, *Opt. Mater.* **2015**, *42*, 381.
- 29 A. Paul, J. D. Donaldson, M. T. Donoghue, M. J. K. Thomas, *Phys. Chem. Glasses* **1977**, *18*, 125.
- 30 D. Benne, C. Rüssel, M. Menzel, K. D. Becker, *J. Non-Cryst. Solids* **2004**, *337*, 232.
- 31 J. A. Duffy, *Geochim. Cosmochim. Acta* **1993**, *57*, 3961.